ELSEVIER

Contents lists available at ScienceDirect

Earth and Planetary Science Letters

www.elsevier.com/locate/epsl



Temporal variations in the composition of Cretaceous Cordilleran arc volcanism through a high-frequency record of bentonites



Sydney Allen a,*, Cin-Ty Lee a, Daniel Minisini a,b

- ^a Dept. of Earth, Environmental and Planetary Sciences, Rice University, MS-126, 6100 Main Street, Houston, TX 77005, USA
- ^b Shell Houston Technological Center, 3333 Highway 6 South, Houston, TX 77082, USA

ARTICLE INFO

Article history: Received 3 September 2021 Received in revised form 11 February 2022 Accepted 22 February 2022 Available online xxxx Editor: R. Hickey-Vargas

Keywords: continental arc volcanism bentonite volcanic compositional episodicity Eagle Ford Group volcanic tempos

ABSTRACT

Continental arc volcanism generates a wide diversity of magma compositions, but the tempos of compositional variation are unclear. Here, we investigate a 7-million year record of volcanic ash layers in the Cretaceous Eagle Ford Group, which was deposited in the Western Interior Seaway in western North America, Low oxygen conditions prevented significant bioturbation, allowing for the preservation of hundreds of thin volcanic ash layers in the form of bentonites. A drill core with an established highresolution age model provides an opportunity to investigate temporal changes in ash composition on <100 kyr timescales. Because of intense alteration during diagenesis, ash protolith compositions were reconstructed from Ti/Zr. We first show that Ti and Zr had limited mobility during diagenesis. We then show, based on a compilation of data from unaltered volcanic rocks from six continental arcs, that the relationship between Ti/Zr and SiO2 is similar across continental arcs from different times and geographic locations, confirming that Ti/Zr is a robust differentiation index and indirect measure of SiO₂, Applying an empirical Ti/Zr-SiO₂ relationship to Ti/Zr measurements of 52 Eagle Ford bentonites allowed for reconstruction of ash protolith SiO2. Ash compositions vary from basalt/basaltic andesite to dacite/rhyolite, but the variations are not random. Ash compositions fluctuate between periods of high silica (>60 wt. % SiO₂) and low silica (<60 wt. %) volcanism over \sim 100 kyr timescales. If the temporal variability of these ashes represents broad snapshots of the Cordilleran continental arc, these results suggest that continental arc systems may undergo episodic changes in the extent of magmatic differentiation or the nature of eruption on rapid (<100 kyr) timescales.

© 2022 Elsevier B.V. All rights reserved.

1. Introduction

Subduction zone volcanism exhibits the largest diversity of compositions in any geologic setting, ranging from basalts to rhyolites (Gill, 1981; Keller et al., 2015; Farner and Lee, 2017). This
compositional diversity is largely controlled by the different extents of magmatic differentiation and mixing, the result of a complex interplay between the dynamics of magma transport, emplacement, and heat loss. These processes are in turn influenced
by many factors, including crustal thickness, tectonic stress, magmatic flux, and erosion (Farner and Lee, 2017). These modulating
factors should vary with time, so despite how diverse arc magmas
are, temporal variations in the average composition of any given
arc or what is erupted might be expected.

Previous studies on the plutonic systems of the Cretaceous Cordilleran continental arc in western North and South America suggest that magmatism at continental arcs varies in tempo and composition over time. These studies have argued for magmatic cyclicity on timescales of 20-80 Myr based on fluctuations in interpreted magmatic flux and isotopic compositions of the rocks (e.g. DeCelles et al., 2009; Ducea et al., 2015; Kirsch et al., 2016; Cecil et al., 2018). Assessing the magnitude and tempos of compositional change in volcanic systems is an important complementary step towards understanding the causes of volcanism, assessing the relationship between plutonic and volcanic systems, and predicting its diverse impacts on climate, natural hazards, ash-driven nutrient fluxes, and other processes.

Creating a high-resolution record (10s-100s of kyr) of volcanic compositions is limited by the number of volcanic units that are preserved and exposed, as well as by the accuracy to which these units can be dated. To help circumvent these challenges, we investigated distal deposits of altered volcanic ash (bentonites) in a sedimentary basin behind the magmatic arc. Although the proximal volcanic units have been removed by erosion, this sedimentary basin preserves a more continuous record of tephra deposition. Here, we investigate a bentonite-rich section within the Cretaceous

^{*} Corresponding author.

E-mail address: sydney.m.allen@rice.edu (S. Allen).

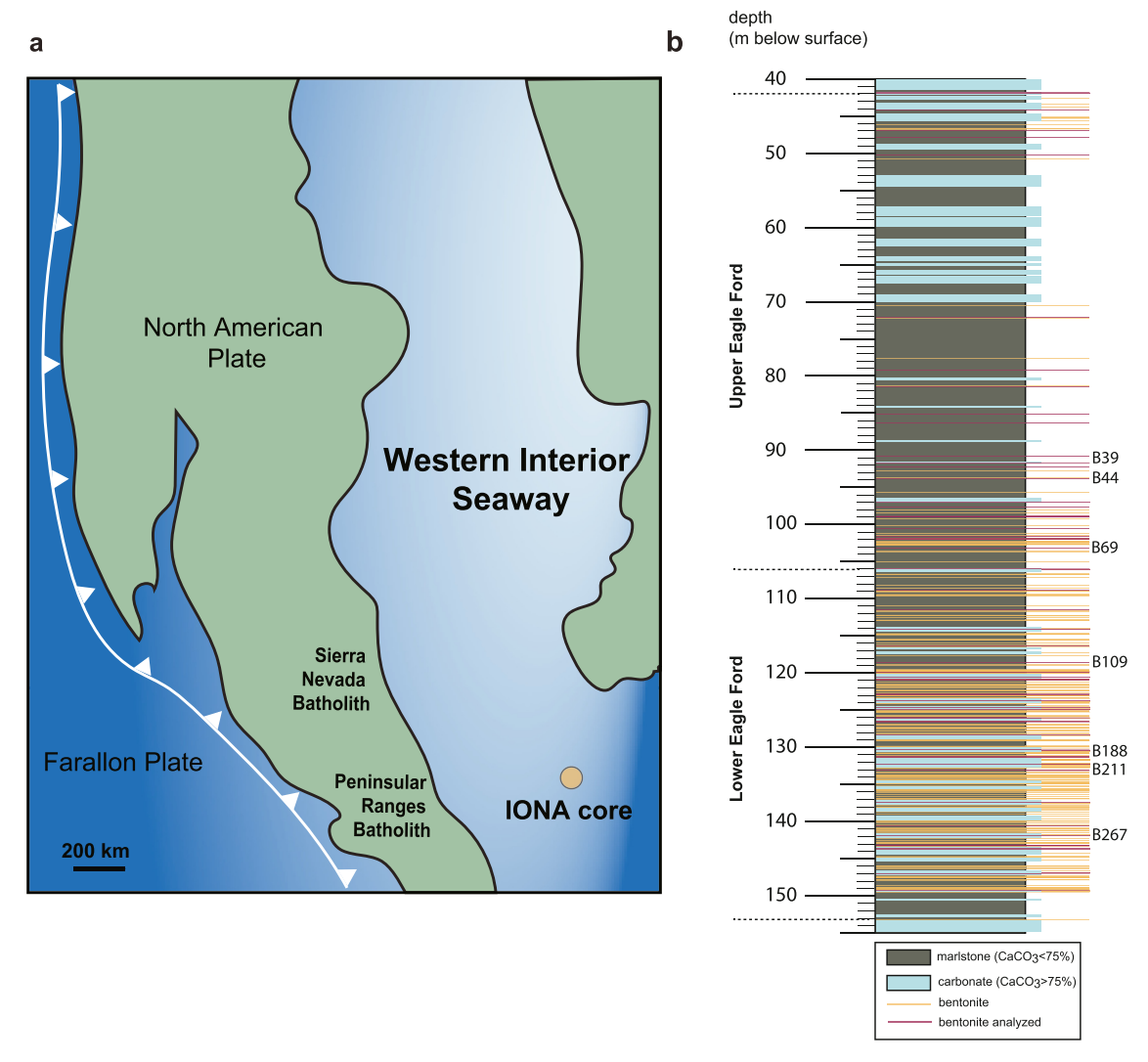


Fig. 1. a. Map showing the approximate locations of the Western Interior Seaway and Iona-1 sediment core in the middle Cenomanian, after Minisini et al., 2018. Volcanic ash was deposited in the shallow epicontinental Western Interior Seaway. Bentonite samples in this study are from core Iona-1 (29°13.51′N, 100°44.49′W). b. The Iona-1 core recovered the entire Eagle Ford Group, which is bounded by the Austin Chalk above and the Buda Limestone below. The upper bentonite sampled in this study is from the Austin Chalk; all others are from the Eagle Ford Group. Bentonites are encased by carbonates and marlstones. For this diagram, carbonates are defined by samples with >75 wt.% CaCO₃ reported by Eldrett et al., 2015a,b, and marlstones are defined by CaCO₃ < 75 wt.%. In outcrops, bentonites typically are recessed, but are shown as extended lines for emphasis. Magenta bentonites are those sampled in our study, which include 52 bentonites that were analyzed with LA-ICP-MS and 4 that were mapped with μ XRF. Bentonites from Figs. 2 and 3 are labeled; depths of the other bentonites analyzed are reported in Table 1. (For interpretation of the colors in the figure(s), the reader is referred to the web version of this article.)

North American Western Interior Seaway (Fig. 1; Lee et al., 2018; Minisini et al., 2018). The bentonites in this section represent altered ash from the Cordilleran magmatic arc and are exceptionally well preserved due to a lack of bioturbation. We combine a high-resolution age model from previous studies with new analyses of 52 bentonites to create a detailed record of volcanic composition over a 7 Myr interval of the late Cretaceous (90-97 Ma), providing a unique opportunity to investigate temporal variability in volcanic composition over sub-million year timescales.

1.1. Case study of bentonites from the Eagle Ford Group

We investigated altered ash beds (bentonites) of the late Cretaceous Eagle Ford Group from the Iona-1 core drilled by Shell Oil in west Texas. The Eagle Ford was deposited in the epicontinental Western Interior Seaway during Cenomanian and Turonian times (Fig. 1). The seaway represented a shallow, dynamically subsiding basin east of the Cretaceous Cordilleran magmatic arc (Liu et al., 2011). In the west Texas region, the physiography of the seaway

minimized siliciclastic inputs, but because of the shallow depths (100-200 m; Eldrett et al., 2015a,b), there was extensive carbonate deposition manifested in the form of limestone-marlstone couplets (Eldrett et al., 2015a,b; Minisini et al., 2018). Carbonates are interbedded with bentonite layers, formed from the alteration of volcanic ash. The Eagle Ford Group records the entire duration of Oceanic Anoxic Event 2 (from 95.01 to 94.05 \pm 0.12 Ma, 112.45-91.74 m in core Iona-1: Sullivan et al., 2020). Anoxic depositional environments during this time allowed for preservation of high amounts of organic matter, making the Eagle Ford an attractive source rock unit for hydrocarbon research. Across the Eagle Ford Group, approximately 290 bentonites have been identified and are on average 3 cm thick (Minisini et al., 2018). In the lower Eagle Ford, when anoxia or dysoxia at the seafloor was common, bentonite preservation was excellent as evidenced by the presence of many thin (<cm-scale) bentonite layers. In contrast, the upper Eagle Ford (rocks vounger than \sim 93.5 Ma) shows more evidence of bioturbation and less organic carbon preservation, presumably due to increasingly oxic conditions. Only the thickest (>3 cm)

bentonite layers appear to be preserved in the upper Eagle Ford, suggesting that thinner layers may have been disturbed by benthic fauna.

Previous studies on the Iona-1 core combined U-Pb dating of volcanic zircons in the bentonites with isotope stratigraphy, biostratigraphy, and cyclostratigraphy to create an integrated age model with high-resolution absolute ages (Eldrett et al., 2015a,b; Minisini et al., 2018). Uncertainties in this astronomically tuned age model are ~40 kyr, providing a rare opportunity to study ashes at a high age resolution.

In most cases, we were unable to sample intact contacts between the bentonite layers and the encasing marlstones because the bentonite layers were too thin or the contacts were too friable. However, we successfully examined contacts for four samples. These were analyzed by µXRF mapping (micro-x-ray fluorescence) to map the distribution of elements across the boundaries, allowing us to assess elemental mobility during diagenesis. One bentonite preserves both the upper and lower contacts, one bentonite preserves the upper contact only, and two bentonites preserve the lower contact only. All other samples were chosen for bulk compositional analysis only and consist of slightly disaggregated chips of bentonites without contacts. For bulk analysis, 52 bentonites were analyzed by LA-ICP-MS (laser ablation inductively coupled plasma mass spectrometry). For these analyses, exact depth and orientation within the bentonite layer was typically not determined. Samples were selected to cover the temporal window of interest as evenly as possible, with care taken to ensure that samples selected had minimal sulfides or other alteration products visible on the surface. The youngest bentonite is from the overlying Austin Chalk rather than the Eagle Ford, but is included as it was visually and compositionally similar to the Eagle Ford bentonites below it. Of the 52 samples used in this study, 42 are from 0-5 cm thick bentonites and 8 are from >10 cm thick bentonites, with a maximum thickness of 64 cm.

Proposed sources of the volcanic ash have included the North American Cordilleran volcanic arc, the Balcones Igneous Province of Texas, and volcanism in southern Arkansas (Pierce et al., 2016). However, recent age estimates do not suggest temporal overlap between the Balcones Igneous Province and Eagle Ford bentonites (Miggins et al., 2004; Griffin et al., 2010). Additionally, the silica undersaturated Balcones volcanism (Griffin et al., 2010) and the lamproites of Arkansas (Zartman, 1977) are inconsistent with the mineralogy of Eagle Ford bentonites, which contain volcanic quartz and zircons. Arc magmatism occurring to the west forms a much more likely source, as there are coeval plutons of a similar composition (e.g. Saleeby et al., 1987; Kistler et al., 2003; Lackey et al., 2008). Additionally, bentonites further north in the seaway have been linked with the Cordilleran arc (Elder, 1988), making Cretaceous Cordilleran volcanism the likely source of the bentonites.

1.2. Prospects and challenges of studying bentonites

Bentonites form due to hydrothermal or diagenetic alteration of volcanic ash (Christidis and Huff, 2009). As a result of intense alteration, they characteristically have a high fraction of smectite-group minerals and are variably enriched or depleted in certain elements, depending on elemental mobility and seawater chemistry (Christidis and Huff, 2009). Ash-water interactions in the Western Interior Seaway produced ideal conditions for bentonite formation. Because of element mobility during bentonite formation, the compositions of bentonites are transformed from the original ash protolith. As a result, inferences about chemical composition of the ash protolith from bentonites must rely on elements that are immobile during diagenesis. However, various studies of bentonites have arrived at differing lists of which elements are immobile, as elemental mobility depends on conditions such as pH, redox con-

ditions, temperature, and salinity (Namayandeh et al., 2020). Thus, mobility of various elements must be assessed on a case-by-case basis. Elements such as Si and Mg are largely agreed to be mobile (e.g. Christidis, 1998; Namayandeh et al., 2020), while rare earth elements and Y have been regarded as immobile in some studies (Winchester and Floyd, 1977) and mobile in others (Kiipli et al., 2017), and Al, Ti, Zr, Nb, and Ta are commonly cited as immobile elements (e.g. Winchester and Floyd, 1977; Christidis, 1998; Kiipli et al., 2017).

Among this family of relatively immobile elements, Ti and Zr are of particular interest as their relative abundances also provide information about magmatic processes (Winchester and Floyd, 1977; Pearce and Norry, 1979; Pearce et al., 1984). Thus, Ti and Zr have been used for the interpretation of a wide range of altered volcanic rocks, including bentonites (e.g. Christidis, 1998; Christiansen et al., 2015; Kiipli et al., 2017; Lee et al., 2018; Hannon et al., 2021). A relationship between Zr/Ti and SiO₂ across different geologic settings led Winchester and Floyd (1977) to suggest this ratio as a differentiation index. In magmas, Ti/Zr varies with extent of differentiation because 1) Zr behaves incompatibly and therefore increases in the residual magmas with progressive crystallization (Lee and Bachmann, 2014) and 2) Ti is removed early in the differentiation process through precipitation of Ti-bearing oxides (Tang et al., 2019). As both elements are widely considered immobile during diagenesis/weathering and contain information about magma petrogenesis, both Christiansen et al. (2015) and Lee et al. (2018) have used the relationship of these elements in unaltered plutonic and volcanic rocks to interpret the protolith composition of bentonites, an approach that we build upon. Here, we 1) test the robustness of Ti and Zr immobility in Eagle Ford bentonites, 2) develop a framework to use Ti/Zr as a differentiation index by examining global systematics between Ti/Zr and SiO₂ in continental arc volcanism, and 3) reconstruct bentonite protolith compositions from measured Ti/Zr.

2. Methods

2.1. Geochemistry of bentonites

Major element intensity maps were created for the four core samples that contained one or both contacts between the bentonite and the encasing marlstone. Maps were determined using a Horiba XGT 7000 μXRF element mapper at Rice University. Analyses were done with a tube diameter of 50 μm , a process time of 6 seconds, and a voltage of 50 kV. Elemental maps were imported into the ImageJ software for post-processing to create false color maps and transects of elemental intensity with depth in the bentonite.

LA-ICP-MS was performed on chips of 52 bentonites with a 213 nm New Wave laser and a Thermo Element 2 ICP-MS at Rice University. For each sample, approximately 3-6 spots were measured at low mass resolution (m/ $\Delta m \sim 300$) and 3-6 at medium mass resolution (m/ $\Delta m \sim 300$), following the methods of Jiang et al. (2015). No significant differences were observed between the Ti or Zr measurements of the two mass resolution modes. Results were calibrated with two external standards, BHVO2g and NIST-610. Spot size diameters of 80 μm were used to ensure homogeneity, as bentonite grains were typically of clay size fraction.

2.2. Global arc dataset

Compositional data for six continental arcs were extracted from precompiled files on the GEOROC database (Aleutian Arc, Andean Arc 1 and 2, Cascade Arc, Central American Arc, Kamchatkan Arc, and New Zealand, Supplemental Table 1, references within) to quantify the global relationship between Ti/Zr and SiO₂. Samples

were filtered to contain only volcanic whole rock compositions with major oxide totals between 97-103% (to avoid altered samples or poor analyses), SiO₂ between 45-80 weight % (to match the typical range of arc volcanic rocks), and Ti/Zr < 130 (due to the low correlation of Ti/Zr with SiO₂ at high Ti/Zr). The filtered dataset included 1842 samples from the Aleutians, 5172 from the Andes, 2813 from the Cascades, 2662 from Central America, 2211 from Kamchatka, and 3137 from New Zealand. For each arc, we performed a least squares regression fit of the data to a polynomial function. To define the global relationship between Ti/Zr (ppm/ppm) and SiO_2 (wt.%), the six data sets (total n = 18724) were also combined and averaged into bins of 0.25 Ti/Zr units. As each arc contains a different number of data points, a weighted average was used to quantify the average SiO2 for each bin of Ti/Zr values. Points were weighted corresponding to the arc they came from to give each of the six arcs an equal impact on the general regression. A general equation to describe the relationship between Ti/Zr and SiO₂ was developed from a least squares regression of the weighted average of each Ti/Zr bin (see Results).

3. Results

3.1. Spatial variation within Eagle Ford bentonites

Four bentonites (B188, B214, B272, B273) were mapped with µXRF to reveal spatial variations in bulk bentonite chemistry (Fig. 2, Supplemental Figures S1-S3). Bentonite B188 preserves both upper and lower contacts (Fig. 2), and displays high Fe and low Ca with respect to the surrounding marlstones. The lower boundary is clearly demarcated in the transects by a sharp transition in Ti (Fig. 2e). In contrast, Al and Si intensities across both boundaries are more diffuse. Ca slightly increases and Ti decreases upwards in the bentonite, but a clear boundary is still evident in the Ca and Ti profiles at the upper contact even though the magnitude of the difference between bentonite and marlstone at the upper contact is smaller than that of the lower contact. These features in B188 are representative of the other bentonites analyzed (Supplemental Figures S1-S3). Importantly, while the sharpness of the boundaries differs slightly between samples and between upper and lower boundaries, Ti profiles are always much sharper than Si and as sharp or sharper than Al profiles across the contacts

Bivariate plots show the covariance of Zr/Ca and Ti/Ca in LA-ICP-MS spots from 52 bentonites (Fig. 3, Supplemental Figures S4-S49). Calcium is used for normalization as it accounts for dilution effects associated with different fractions of carbonate, which does not contain Ti or Zr. Two elements that are perfectly immobile or have exactly the same geochemical behavior during diagenesis should define a linear correlation that intersects the origin. To evaluate immobility with this approach, linear regressions were performed with and without forcing the regression through the origin. For most bentonites, the slopes of regressions are similar for both regression scenarios (Table 1). When the regressions are forced through zero, the slopes, which are one method of establishing bentonite Ti/Zr, range from 9.2 to 120.5. When Ti/Zr is estimated by averaging the Ti/Zr of all spots analyzed in a sample, Ti/Zr is between 9.3 and 116.2

We note that linear regressions of Zr/Ca and Ti/Ca for a small subset of samples do not produce high correlation coefficients and have intercepts that are slightly offset from the origin. These samples tend to be those with very low Ti/Ca and Zr/Ca, or samples in which ratios are very tightly clustered. However, the general Ti/Ca and Zr/Ca coupling across a wide range of magnitudes in other samples justifies the assumption of Ti and Zr immobility.

Many samples display a larger range of values, reflecting spatially variable compositions. As we do not know the orientation or depth of most sample chips with respect to the bentonite bed, it is unclear whether compositional variations occur laterally or vertically within a bentonite. Slopes, intercepts, and r^2 values are reported for each bentonite (Table 1). While the slopes of the regression lines, e.g. Ti/Zr, vary for different bentonites and hence across stratigraphic age, there are no correlations observed between the strength of the fit of the regression line and the thickness, age, or composition of the bentonite.

3.2. Global systematics of Ti and Zr in continental arcs

During magmatic differentiation, Ti/Zr decreases with increasing SiO_2 owing to the incompatible behavior of Zr and the more compatible behavior of Ti associated with metal oxide fractionation (Fig. 4a, Tang et al., 2019). Through our binning and weighting procedure of the six arcs described in the methods section, we arrive at a polynomial regression for the binned data ($r^2 = 0.977$)

$$SiO_2 = -2.456 \times 10^{-5} (Ti/Zr)^3 + 0.007482 (Ti/Zr)^2$$
$$-0.7807 (Ti/Zr) + 78.29$$

where SiO_2 is in wt.% and Ti/Zr is in ppm/ppm. We have taken this regression to be universal for continental arcs as each of the six continental arcs define a similar relationship between Ti/Zr and SiO_2 (Fig. 4b).

An important feature of this regression is its nonlinearity. At high Ti/Zr, variation in Ti/Zr corresponds to small changes in SiO $_2$, implying that SiO $_2$ contents predicted from high Ti/Zr ratios will have high uncertainty. In other words, at high Ti/Zr (low SiO $_2$), the above model loses sensitivity and cannot distinguish between basalts and basaltic andesites. Given the paucity of basalts in continental arc environments, high Ti/Zr likely corresponds to basaltic andesites in our study. We consider the above equation valid for Ti/Zr < 130. This is because of both the limited number of high Ti/Zr samples (corresponding to primitive magmas) for many arc systems and the decrease in sensitivity of the model at high Ti/Zr.

3.3. Temporal variability in Ti/Zr compositions

Measurements of Ti/Zr from LA-ICP-MS were combined with the age model of Minisini et al. (2018) to assess temporal changes in volcanic composition (Fig. 5a). Over the interval 97-90 Ma, there were periods characterized by ash with high Ti/Zr and periods characterized by low Ti/Zr. The oldest million-year interval, except for one bentonite, has low Ti/Zr, followed by a half million-year period with generally higher Ti/Zr. The four bentonites with the highest Ti/Zr occur within a 200 kyr period centered at 94.5 Ma, suggesting relationships between time and magma composition.

Using our empirical equation relating Ti/Zr and SiO₂ in arc magmas and the average Ti/Zr of LA-ICP-MS spots for each bentonite, we reconstructed the original SiO₂ of each ash layer before it was altered into bentonite (Fig. 5b). Reconstructed compositions demonstrate a large magnitude of compositional variability, ranging from basaltic/basaltic-andesite to dacitic/rhyolitic compositions. Bentonites in close age proximity (within 1-10 kyr) typically have similar compositions, such as those centered near 96 Ma and 94.5 Ma, but large changes in SiO₂ also may have occurred over short timescales, such as the rapid shift between four tightly spaced basaltic eruptions to two overlapping dacite-rhyolite eruptions between 94.3 and 94.6 Ma. The lower number of preserved bentonites in the youngest three million years prevents accurate assessment of short-timescale compositional variability in this part of the section.

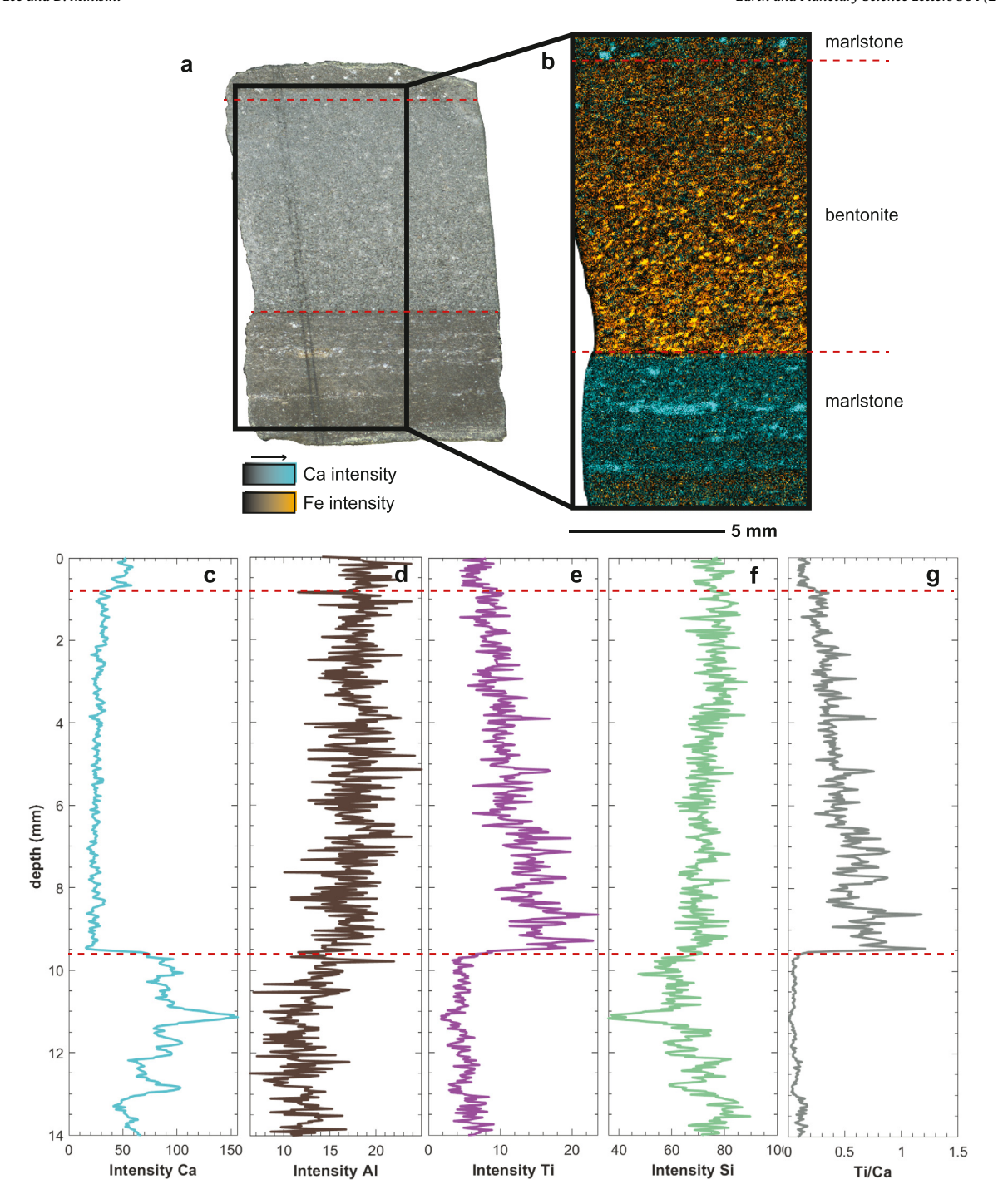


Fig. 2. μXRF of bentonite B188. a. Scanned image of the bentonite bounded by marlstones in the Iona-1 core. Boundaries between the bentonite and marlstones are shown by dotted red lines. b. False color map from XRF counts of Ca and Fe for the boxed region of a. c-g. Transects of grayscale intensities of XRF maps of Ca, Al, Ti, Si, and Ti/Ca. Each point in the curves represents the average grayscale intensity of a horizontal row of pixels in the μXRF map.

4. Discussion

4.1. Evaluating the robustness of ash protolith reconstructions

The sharp lower boundary in the Ti profile of bentonites supports the assumption that Ti is immobile or of low immobility in Eagle Ford bentonites (Fig. 2, Supplemental Figures S1). While Al is commonly cited as immobile or of low mobility, the more diffuse profile of Al across the lower boundary of bentonite B188 suggests that some amount of Al diffused across the boundary after deposition. We thus chose Ti as an indicator of original contents of the support of the

nal ash composition. The very diffuse profiles of Si suggest that, as expected, Si is affected by diagenetic alteration and should not be used directly for the interpretation of primary ash chemistry.

The strength of the linear relationship between Zr/Ca and Ti/Ca (Fig. 3) justifies our assumption of immobility for both elements and points towards two-component mixing between ash and carbonates. Even in the cases in which there is evidence of significant mixing, indicated by a large range of Ti/Ca or Zr/Ca, the regression intercept is typically very close to the origin, suggesting that the ash was mixing with a source that did not contain significant Ti or

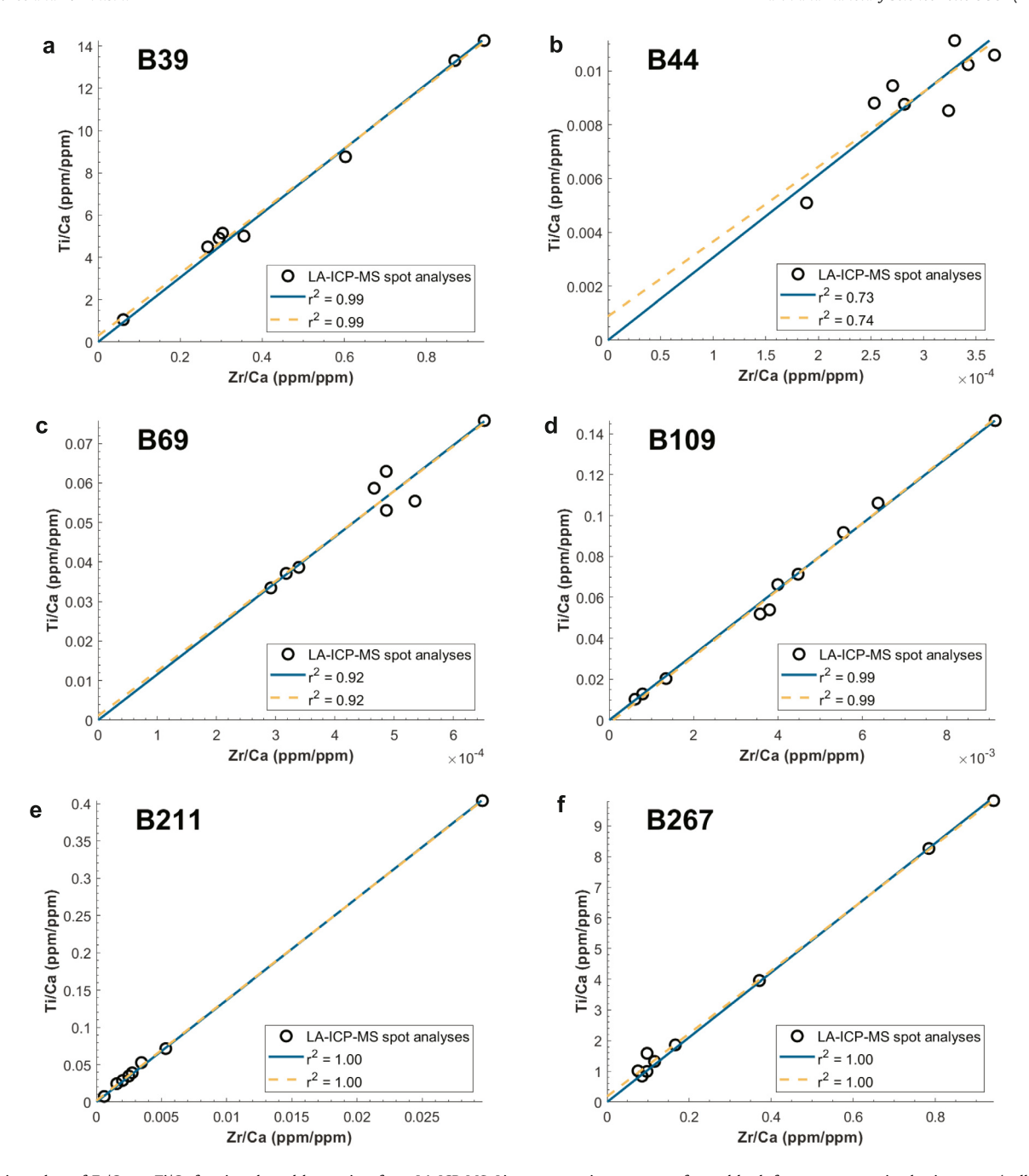


Fig. 3. Bivariate plots of Zr/Ca vs. Ti/Ca for six selected bentonites from LA-ICP-MS. Linear regressions were performed both for an unconstrained y-intercept (yellow) and for a y-intercept set to 0 (blue). Regression lines that pass through 0 with high r^2 values show the strongest evidence of Ti and Ti immobility. Samples were chosen for display across the temporal window studied. Samples were additionally chosen to show that strong linear relationships exist for Ti/Ca and Ti/Ca across three orders of magnitude. Low correlation coefficients, such as in B44, are most common for samples with very low Ti/Ca and Ti/Ca, and result in linear regression lines that intersect the y- or x-axes at points other than the origin. Bivariate plots for the remaining 46 samples are in supplementary Figures S4-S49.

Zr. Therefore, we infer that the Ti/Zr ratio has not been appreciably contaminated by siliciclastics.

Ash has experienced significant and variable dilution with carbonates, with Ti/Ca varying over 3 orders of magnitude between samples. Differences in Ti/Ca within single samples may result from the position of the analysis spot with respect to the marlstone, as μXRF shows that Ti/Ca varies with depth in the bentonite (Fig. 2). However, these samples with a large range in Ti/Ca and Zr/Ca generally have regression lines that pass through or near the origin with strong correlation coefficients, suggesting that physical carbonate dilution processes did not impact the Ti/Zr of our bentonites and that Ti/Zr is a good descriptor of the bentonites independent of factors such as depth in the bentonite.

4.2. Comparison of Eagle Ford bentonites with Cretaceous Cordilleran Batholiths

The reconstructed ash compositions of our 52 bentonites were compared with plutonic compositions from the California segment of the Peninsular Ranges Batholith (PRB) reported by Lee et al. (2007) and with plutonic samples from the Sierra Nevada Batholith (SNB; data downloaded from EarthChem; references available in Supplementary Table 3). Peak magmatism of the PRB broadly coincides with the age range of the bentonites, and the Sierra Nevada experienced a major pulse of magmatism at this time. The PRB and SNB are the nearest coeval Cordilleran batholiths to the Eagle Ford, making them potential plutonic counterparts to the ben-

Table 1List of 52 bentonites studied here. Ages are from the models of Eldrett et al., 2015a,b and Minisini et al., 2018, and depths and thicknesses are from Minisini et al., 2018.

Bentonite	Age (Ma)	Depth (m below surface)	Thickness (cm)	Number of spots	Ti/Zr	σ Ti/Zr	Inferred SiO2	Slope	Intercept	R ²	Slope (through 0)	R ² (through 0
14	90.271	41.87	13	8	31.08	3.41	60.2	35.57	-0.0017	0.92	32.05	0.91
15	90.324	42.62	8	9	23.92	3.58	63.4	25.84	-0.0029	0.91	24.76	0.91
18	90.46	44.28	3	8	28.15	2.43	61.4	30.55	-0.0006	0.81	28.3	0.8
26	90.7	46.95	2	9	38.92	4.3	57.4	33.31	0.02	0.95	36.28	0.94
27	90.728	47.9	64	6	31.04	4.29	60.2	28.01	0.0074	0.97	29.5	0.97
28	90.893	50.24	22	10	19.52	1.85	65.6	18.25	0.012	0.86	19.44	0.86
31	92.838	72.11	10	8	19.1	3.82	65.9	24.24	-0.079	0.59	19.51	0.57
34	93.197	79.3	2	7	24.79	2.58	62.9	23.52	0.0001	0.68	24.73	0.68
36	93.327	81.5	19	8	37.28	12.07	58.1	53.1	-0.043	0.9	42.48	0.85
37	93.585	85.28	1	7	34.95	3.5	58.9	34.3	0.0012	0.98	34.89	0.98
38	93.664	86.46	3	8	37.76	4.05	58	35.33	0.022	0.99	36.34	0.98
39	93.92	90.87	3	8	15.86	1.21	67.9	14.79	0.29	0.99	15.24	0.99
40	93.97	91.8	2	8	17.76	1.5	66.8	15.68	0.001	0.95	17.26	0.94
41	93.997	92.34	2	8	76.25	22.86	51.3	107.2	-0.07	0.89	88.5	0.86
44	94.074	93.93	1	8	30.83	3.4	60.4	27.79	0.0009	0.74	30.69	0.73
46	94.233	97.12	1	9	67.71	11	52.1	65.96	0.001	0.83	66.2	0.83
47	94.265	97.75	2	8	23.32	2.51	63.8	20.92	0.0023	0.88	22.93	0.87
50	94.334	98.97	3	8	9.25	0.73	72.3	8.42	0.01	0.92	9.15	0.92
51	94.34	99.07	3	8	10.87	0.95	71.2	11.99	-0.013	0.95	11.04	0.94
54	94.417	100.59	14	8	84.21	31.57	50.8	68.74	0.076	0.45	82.51	0.43
57	94.474	101.73	5	9	105.63	21.13	50	141.6	-0.0021	0.97	120.48	0.94
58	94.484	101.97	1	8	94.13	8.5	50.3	41.78	0.021	0.53	92.6	-0.27
69	94.547	103.23	5	8	116.16	8.33	49.7	113.66	0.0011	0.92	115.92	0.92
73	94.684	106.06	1	7	61.18	9.53	52.9	55.33	0.018	0.93	58.57	0.93
79	94.819	108.93	2	7	43.19	5.45	56.4	37.88	0.0013	0.94	41.47	0.93
87	94.953	111.505	0.5	6	19.36	1.9	65.9	22.97	-0.0009	0.77	19.51	0.76
96	95.101	114.21	1	10	28.47	3.33	61.4	21.17	0.016	0.67	27.98	0.6
105	95.22	116.44	3	8	13.9	1.42	69.1	10.1	0.065	0.9	13.4	0.8
109	95.323	118.69	10	10	15.85	0.91	67.9	16.32	-0.0016	0.99	16.04	0.99
118	95.38	119.88	1	9	17.75	1.16	66.8	14.53	0.077	0.97	17.26	0.93
122	95.418	120.63	1	8	71.71	10.82	51.7	67.95	0.009	0.98	69.8	0.98
124	95.435	120.97	1	8	55.08	4.04	53.8	43.04	0.064	0.95	53.54	0.89
135	95.524	122.71	2	9	27.68	2.36	61.7	25.87	0.0078	0.97	26.76	0.97
144	95.578	123.8	3	8	59.12	10.82	53.2	74.43	-0.026	0.94	62.7	0.91
152	95.622	124.73	18	10	20.35	2.22	65.3	18.6	0.012	0.97	19.51	0.97
154	95.633	125.03	1	6	42.49	4.65	56.6	27.78	0.11	0.8	41.26	0.6
161	95.683	126.001	3	10	42.82	4.64	56.5	37.26	0.1	0.95	40.77	0.94
166	95.717	126.69	4	8	51.24	26.26	54.5	67.04	-0.085	0.58	61.01	0.57
177	95.805	128.45	3	6	48	4.77	55.2	37.19	0.018	0.82	46.82	0.76
184	95.898	130.23	9	10	32.67	4.82	59.7	27.81	0.045	0.84	31.84	0.82
193	95.948	131.34	1	9	16.92	1.63	67.2	17.54	-0.0027	0.97	17.25	0.97
201	95.993	132.277	0.3	8	14.37	1.22	68.8	13.84	0.0055	0.91	14.32	0.91
211	96.037	133.13	5	8	14.14	1.05	69	13.58	0.0018	1	13.67	1
241	96.265	137.5	2	9	9.43	1.47	72.2	12.27	-0.054	0.95	10.19	0.92
258	96.428	140.63	7	7	15.9	1.77	67.9	15.36	-0.014	1	15.21	1
267	96.497	142.061	6	9	11.59	2.07	70.7	10.25	0.18	1	10.54	1
272	96.537	143.01	0.5	7	44.15	7.11	56.1	28.38	0.16	0.4	43.42	0.28
272	96.552	143.27	5	10	15.9	1.41	67.9	14.54	0.061	0.97	14.93	0.28
275 275	96.563	143.507	4	8	15.21	1.41	68.3	16.81	-0.0003	0.57	15.37	0.57
273 277	96.577	143.8	9	11	21.27	5.43	64.8	19.45	0.0003	0.77	20	0.77
287	96.732	147.015	0.5	8	22.51	2.71	64.2	18.69	0.64	0.94	20.67	0.93
301	96.844	149.243	0.2	8	23.65	2.71	63.6	22.6	0.04	0.94	23.42	0.98

tonites (Fig. 1). It is possible that the bentonites could derive from multiple Cordilleran sources. Plutonic samples from both batholiths were selected only between 100 and 90 Ma, comparable to the 90-97 Ma represented by our Eagle Ford samples.

Broad similarities are seen between the distributions of compositions from the Eagle Ford and the two batholiths, with the strongest similarities between the Eagle Ford and SNB. For example, 56% of SNB samples have SiO_2 greater than 63 wt.%, compared with 46% of the reconstructed Eagle Ford samples, and 18% of SNB samples fall between 57-63 wt.% SiO_2 , as compared to 23% of Eagle Ford samples. All three distributions have a peak between 64-68 wt.% SiO_2 . The PRB is dominated by samples >57 wt.% during this time (Fig. 6).

There is a narrower compositional distribution for the Eagle Ford than for either of the batholiths, with multiple possible causes. One important consideration is that errors in the regression are greater at high Ti/Zr, corresponding to low SiO_2 . This reflects

the fact that Ti/Zr becomes a less sensitive predictor of SiO₂ below 60 wt.% SiO₂ and that there are fewer samples in our compiled datasets with high Ti/Zr. Therefore, even if ash was derived from eruptive products characterized by <50 wt.% SiO₂, we would be unable to accurately reconstruct its composition from Ti/Zr alone. Another potential reason for this difference is that low silica ash may represent less explosive events and thus may be less likely to produce large volumes of ash to be transported and preserved.

There are many complexities to the volcanic-plutonic connection that make direct comparisons of both records challenging. The volcanic record provides information about the magma system at the time of eruption, while the plutonic record may contain a memory of a long history of magmatic processes (Barnes et al., 2019). Additionally, there may be systematic differences between the compositions of magmas that erupt or stall in the crust (Keller et al., 2015). Due to such complexities, differences between the recorded plutonic and volcanic compositions are to be expected

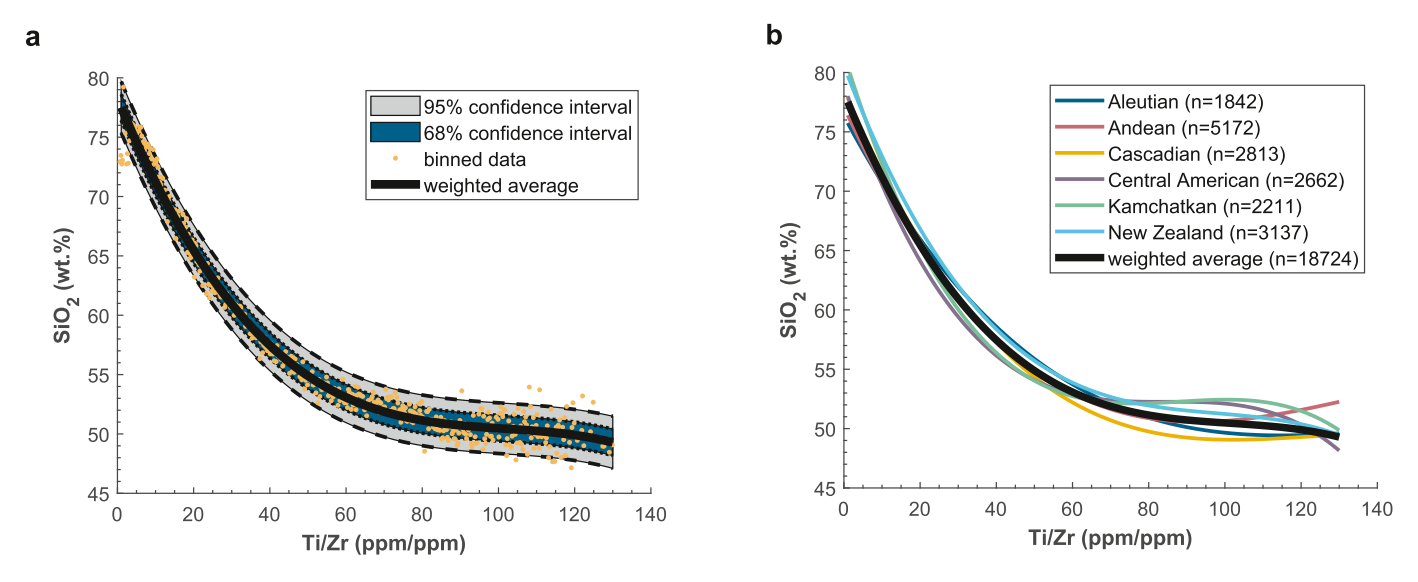


Fig. 4. a. Regression and confidence intervals of compiled data from six continental arcs. Data were binned in units of 0.25 Ti/Zr and assigned weights to equalize the influence of each arc. b. Regressions of six arcs using data that were not binned show the similarity of the relationship between Ti/Zr and SiO₂ for all six arcs. The black line is from the weighted average of a.

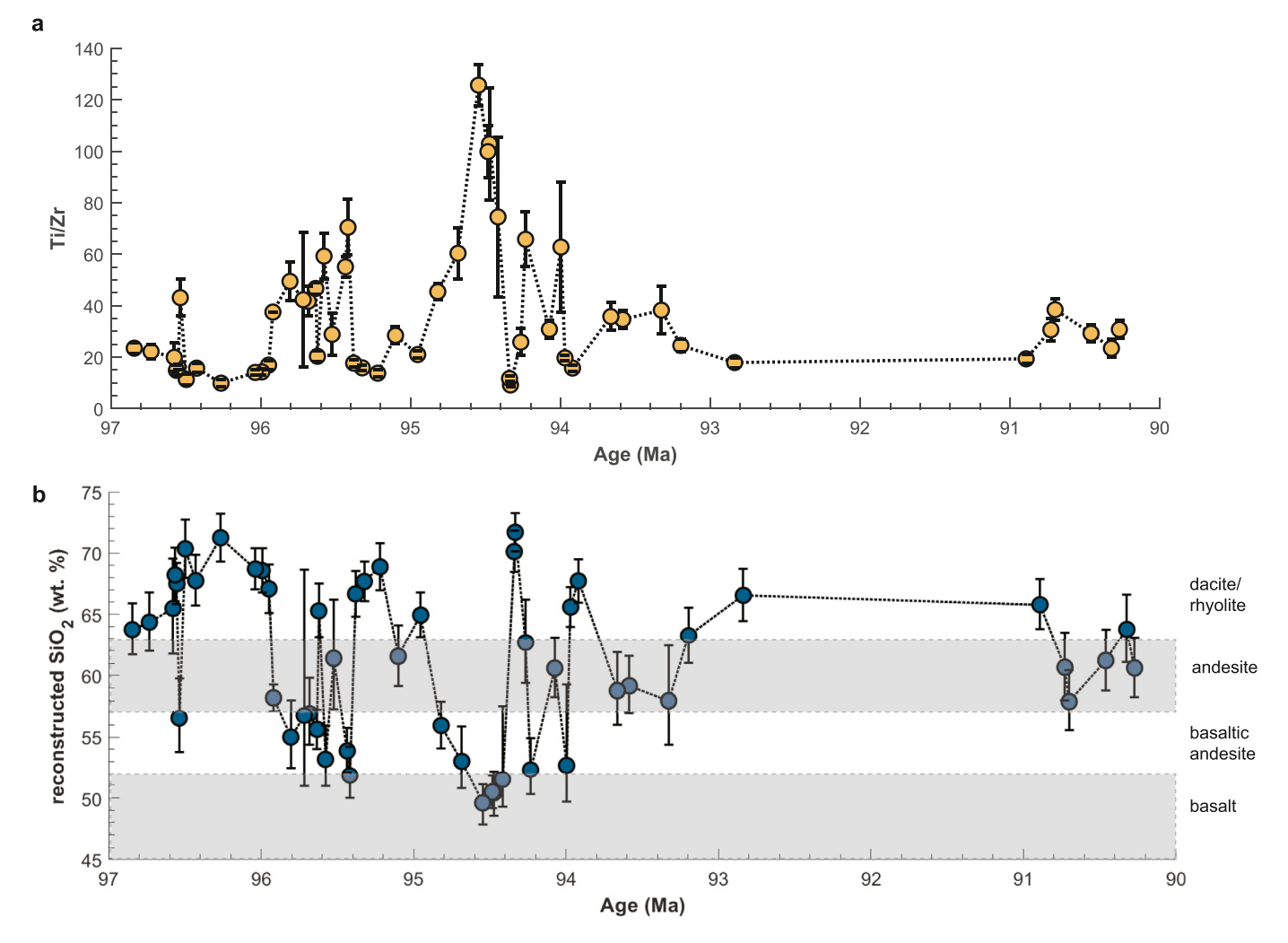


Fig. 5. a. Variations in measured Ti/Zr with age of 52 bentonites. Error bars represent 1σ of Ti/Zr measurements for each sample. b. Reconstructed SiO₂ weight percent for the 52 bentonites using our equation relating Ti/Zr and SiO₂. Error bars represent 1σ in Ti/Zr measurements and 1σ from the regression (Fig. 4a).

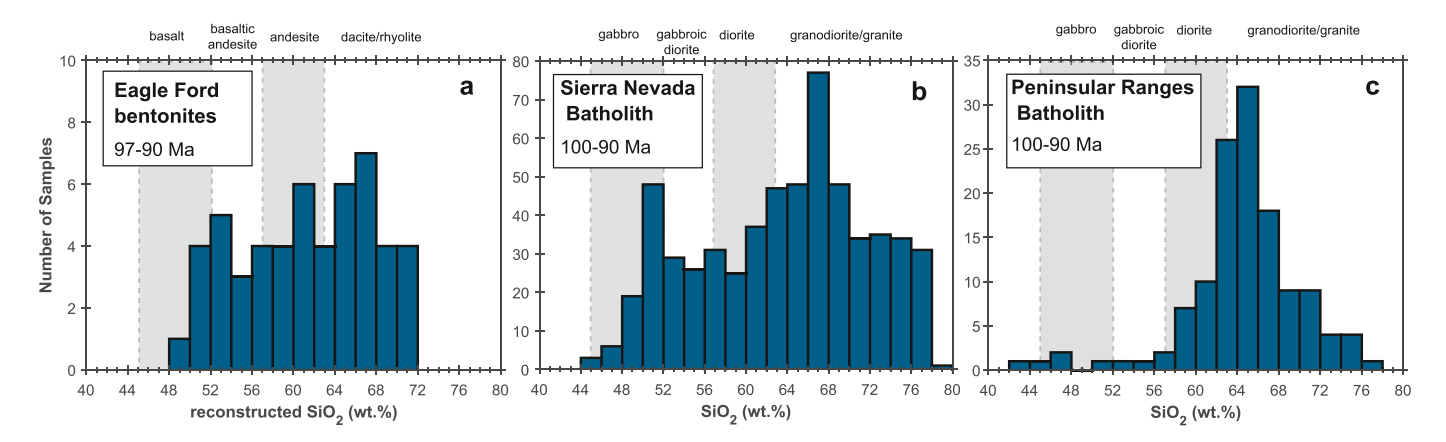


Fig. 6. a. Histogram of reconstructed SiO₂ compositions for 52 Eagle Ford bentonites. b. Histogram of 580 compiled SiO₂ compositions from the Sierra Nevada Batholith. References are included in Supplemental Table 3. c. Histogram of 129 SiO₂ compositions from the Peninsular Ranges Batholith of California, reported by Lee et al. (2007). The Peninsular Ranges Batholith and Sierra Nevada Batholith represent possible plutonic counterparts to the Eagle Ford bentonites, and samples are filtered to contain only compositions that are coeval with the bentonites examined in this study. All distributions are binned by 2 weight percent SiO₂.

(Bachmann et al., 2007). However, despite these differences, the broad similarities in these distributions, especially between the bentonites and the SNB, suggest that the ash preserved as bentonites was derived from a continental arc system rather than from previously proposed intraplate sources. One caveat to be considered is that the Eagle Ford may contain input from multiple sources. This approach is insufficient to determine the direct plutonic counterpart, but does provide evidence that the plutonic counterpart is Cordilleran.

4.3. Temporal variability in arc systems

Many studies of the Cordilleran plutons of North and South America have documented cyclicity or episodicity in both magmatic composition and flux (e.g. DeCelles et al., 2009; de Saint Blanquat et al., 2011; Ducea et al., 2015; Paterson and Ducea, 2015; Kirsch et al., 2016; Cecil et al., 2018, Martínez Ardila et al., 2018). These authors have shown cyclicity in magmatic flux on 20-80 Ma timescales, which can vary along the arc and over time in a system. Proposed drivers of these cycles remain debated, and include changes in motion of the subducting plate or regional stress state (Ducea et al., 2015; Paterson and Ducea, 2015), smallscale upper plate processes (Cecil et al., 2018), compositional or thermal changes in the deep lithosphere (de Saint Blanquat et al., 2011), changes in retroarc shortening producing variations in the availability of crustal melts (DeCelles et al., 2009), mantle input (Martínez Ardila et al., 2018; Attia et al., 2020), or a mixture of the above processes (Kirsch et al., 2016). The many proposed mechanisms driving cyclic changes are a testament to the diversity and complexity of Cordilleran systems and point to the many processes that can impact magma compositions. However, it is important to note that the timescales of observed compositional and volumetric episodicity in Cordilleran plutons are on a different order of magnitude than the sub-million year timescales of episodicity we document in Eagle Ford bentonites.

Past studies of cyclicity and episodicity in volcanic systems have been more limited than those in plutonic systems but have documented changes over shorter timescales. In studies of Cenozoic island arcs, ash reveals 2-5 Myr episodicity in timing of volcanism (Kennett et al., 1977; Cambray et al., 1993). Work on continental volcanic arcs has been limited, but several studies have assessed links between continental arc composition and time, leading to arguments of 2.5 Myr cyclicity of Alaskan ash composition (Scheidegger and Kulm, 1975) and several Myr compositional episodicity in Kamchatkan ash (Scheidegger et al., 1978). One pervasive challenge to these previous studies of temporal changes in volcanism is the

age resolution of the studies. Although large error in ages creates uncertainty in assessing trends in composition and flux, previous studies generally suggest that volcanic timescales of change may be much shorter than plutonic timescales.

Eagle Ford bentonites display compositional changes occurring over short, 100 kyr timescales, indicating rapid fluctuations in volcanism. It is unclear what process or processes can drive these high frequency compositional changes. While previous authors have invoked large-scale processes such as delamination or changes in the rates or direction of plate motion to explain cyclicity in Cordilleran magmatic activity, these tectonic processes would seem to operate too slowly to give rise to such high frequency fluctuations in the composition of magmas at the batholith scale. More plausible on short timescales might be changes in the nature of magmatic and volcanic plumbing systems that may dictate the extent of differentiation experienced by magmas by the time they reach shallow volcanic systems or bias eruptions to a particular magma type. Processes that may change the nature of magmatic plumbing systems include 1) changes in crustal thickness, which may change residence times of magmas in the crust and 2) changes in local stress state, which may influence the extent of magmatic differentiation or the eruptibility of shallow level magmatic reservoirs. The extent of change produced by these processes over 100 kyr timescales remains a question. Nevertheless, we note that recent authors have suggested that changes in loading (from alpine glaciers or changes in sea level) associated with the waxing and waning of ice sheets could cause changes in magmatic flux and composition on \sim 10 kyr timescales (Jellinek et al., 2004; Lund and Asimow, 2011; Crowley et al., 2015). We highlight the effects of direct and indirect glacial loading not because we wish to imply ice sheets existed in the Cretaceous, but rather to draw attention to the possibility that rapid changes in loading may be important. In the case of the Cordilleran arc and foreland fold and thrust belt, one could envision crustal stress states varying rapidly due to changes in the various processes that control loading, that is, the thickness of the crust, erosion rates, sedimentary deposition rates in the back arc, and finally changes in dynamic subsidence (Fig. 7). Unraveling the origins of these rapid compositional fluctuations is beyond the scope of this paper, but we hope that our observations and discussions might inspire future studies.

5. Conclusions

In summary, we demonstrate that bentonites can be useful for interpreting the history of eroded continental arcs, despite the mo-

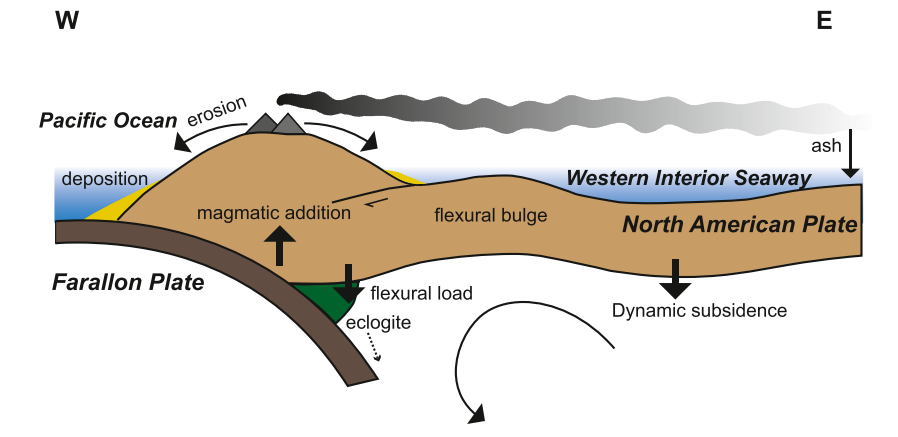


Fig. 7. Cordilleran volcanism deposited ash in the distal Western Interior Seaway. While volcanism was driven by subduction of the Farallon Plate, the causes of compositional variations are unclear. Extent of differentiation and composition may be influenced by factors such as crustal thickness, tectonic stress, and magmatic flux, which in turn are influenced by various tectonic and magmatic processes (see discussion). Figure is not to scale.

bility of elements such as Si. By developing a procedure for ash protolith interpretation and applying this procedure to bentonites of the Cretaceous Eagle Ford Group, we show the compositional diversity of the coeval Cordilleran arc volcanism and create a detailed record of compositional variability with time.

Our approach depends on the use of Ti and Zr, which we argue are largely immobile in our samples. Eagle Ford bentonites have varying amounts of carbonate, but the low mobility of Ti and Zr make Ti/Zr an appropriate descriptor of bentonites. We define a relationship relating Ti/Zr and SiO₂ in continental arc volcanic rocks for Ti/Zr < 130, and demonstrate that this relationship is extremely similar for six continental arcs of different ages across the globe, suggesting that our procedure for bentonite interpretation can be applied to additional arcs. We use the relationship we define between Ti/Zr and SiO₂ to estimate the original composition of ash before it was altered into the Eagle Ford bentonites. and find that ash deposited in this group spanned a large compositional range from basaltic andesite to rhyolite. Some periods were characterized by high silica volcanism, while others were characterized by more mafic volcanism; transitions occurred over timescales of 100s of kyr. Additional work is necessary to understand the drivers of compositional changes over the sub-million year timescales recorded here in bentonites.

CRediT authorship contribution statement

Sydney Allen: Conceptualization, Investigation, Visualization, Writing – original draft. **Cin-Ty Lee:** Conceptualization, Funding acquisition, Supervision, Writing – review & editing. **Daniel Minisini:** Resources, Writing – review & editing.

Declaration of competing interest

The authors declare that they have no known competing financial interests or personal relationships that could have appeared to influence the work reported in this paper.

Acknowledgements

We thank Patrick Phelps and Mark Torres for help in sampling core material. Funding for this work was provided from NSF Award OCE-1338842 to Cin-Ty Lee. S. Allen thanks the Geological Society of America for helping support this research through a student grant in aid of research.

Appendix A. Supplementary material

Supplementary material related to this article can be found online at https://doi.org/10.1016/j.epsl.2022.117470.

References

Attia, S., Cottle, J.M., Paterson, S.R., 2020. Erupted zircon record of continental crust formation during mantle driven arc flare-ups. Geology 48, 446–451. https://doi.org/10.1130/G46991.1.

Bachmann, O., Miller, C.F., de Silva, S.L., 2007. The volcanic-plutonic connection as a stage for understanding crustal magmatism. J. Volcanol. Geotherm. Res. 167, 1–23. https://doi.org/10.1016/j.jvolgeores.2007.08.002.

Barnes, C.G., Werts, K., Memeti, V., Ardill, K., 2019. Most granitoid rocks are cumulates: deductions from hornblende compositions and zircon saturation. J. Petrol. 60 (11), 2227–2240. https://doi.org/10.1093/petrology/egaa008.

Cambray, H., Cadet, J.-P., Pouclet, A., 1993. Ash layers in deep-sea sediments as tracers of arc volcanic activity: Japan and Central America as case studies. Isl. Arc 2, 72–86. https://doi.org/10.1111/j.1440-1738.1993.tb00075.x.

Cecil, M.R., Rusmore, M.E., Gehrels, G.E., Woodsworth, G.J., Stowell, H.H., Yokelson, I.N., Chisom, C., Trautman, M., Homan, E., 2018. Along-strike variation in the magmatic tempo of the coast mountains batholith, British Columbia, and implications for processes controlling episodicity in arcs. Geochem. Geophys. Geosyst. 19, 4274–4289, https://doi.org/10.1029/2018GC007874.

Christiansen, E.H., Kowallis, B.J., Dorais, M.J., Hart, G.L., Mills, C.N., Pickard, M., Parks, E., 2015. The record of volcanism in the Brushy Basin Member of the Morrison Formation: implications for the Late Jurassic of western North America. In: Geological Society of America Special Papers. In: Geological Society of America, vol. 513, pp. 399–439.

Christidis, G.E., 1998. Comparative study of the mobility of major and trace elements during alteration of an andesite and a rhyolite to bentonite, in the islands of Milos and Kimolos, Aegean, Greece. Clays Clay Miner. 46, 379–399. https://doi.org/10.1346/CCMN.1998.0460403.

Christidis, G.E., Huff, W.D., 2009. Geological aspects and genesis of bentonites. Elements 5, 93–98. https://doi.org/10.2113/gselements.5.2.93.

Crowley, J.W., Katz, R.F., Huybers, P., Langmuir, C.H., Park, S.-H., 2015. Glacial cycles drive variations in the production of oceanic crust. Science 347, 1237–1240. https://doi.org/10.1126/science.1261508.

de Saint Blanquat, M., Horsman, E., Habert, G., Morgan, S., Vanderhaeghe, O., Law, R., Tikoff, B., 2011. Multiscale magmatic cyclicity, duration of pluton construction, and the paradoxical relationship between tectonism and plutonism in continental arcs. Tectonophysics 500, 20–33. https://doi.org/10.1016/j.tecto.2009.12.009.

DeCelles, P.G., Ducea, M.N., Kapp, P., Zandt, G., 2009. Cyclicity in Cordilleran orogenic systems. Nat. Geosci. 2, 251–257. https://doi.org/10.1038/ngeo469.

Ducea, M.N., Saleeby, J.B., Bergantz, G., 2015. The architecture, chemistry, and evolution of continental magmatic arcs. Annu. Rev. Earth Planet. Sci. 43, 299–331. https://doi.org/10.1146/annurey-earth-060614-105049.

Elder, W.P., 1988. Geometry of Upper Cretaceous bentonite beds: implications about volcanic source areas and paleowind patterns, western interior, United States. Geology 16, 835–838.

Eldrett, J.S., Ma, C., Bergman, S.C., Lutz, B., Gregory, F.J., Dodsworth, P., Phipps, M., Hardas, P., Minisini, D., Ozkan, A., Ramezani, J., Bowring, S.A., Kamo, S.L., Ferguson, K., Macaulay, C., Kelly, A.E., 2015a. An astronomically calibrated stratigraphy of the Cenomanian, Turonian and earliest Coniacian from the Cretaceous Western Interior Seaway, USA: implications for global chronostratigraphy. Cretac. Res. 56, 316–344. https://doi.org/10.1016/j.cretres.2015.04.010.

- Eldrett, J.S., Ma, C., Bergman, S.C., Ozkan, A., Minisini, D., Lutz, B., Jackett, S.-J., Macaulay, C., Kelly, A.E., 2015b. Origin of limestone-marlstone cycles: astronomic forcing of organic-rich sedimentary rocks from the Cenomanian to early Coniacian of the Cretaceous Western Interior Seaway, USA. Earth Planet. Sci. Lett. 423, 98-113. https://doi.org/10.1016/j.epsl.2015.04.026.
- Farner, M.J., Lee, C.-T.A., 2017. Effects of crustal thickness on magmatic differentiation in subduction zone volcanism: a global study. Earth Planet. Sci. Lett. 470, 96–107. https://doi.org/10.1016/j.epsl.2017.04.025.
- Gill, J.B., 1981. Orogenic Andesites and Plate Tectonics, Minerals and Rocks. Springer Berlin Heidelberg. Berlin. Heidelberg.
- Griffin, W.R., Foland, K.A., Stern, R.J., Leybourne, M.I., 2010. Geochronology of bimodal alkaline volcanism in the Balcones igneous province, Texas: implications for Cretaceous intraplate magmatism in the northern Gulf of Mexico magmatic zone. J. Geol. 118, 1–21. https://doi.org/10.1086/648532.
- Hannon, J.S., Dietsch, C., Huff, W.D., 2021. Trace-element and Sr and Nd isotopic geochemistry of Cretaceous bentonites in Wyoming and South Dakota tracks magmatic processes during eastward migration of Farallon arc plutons. GSA Bull. 133, 1542–1559. https://doi.org/10.1130/B35796.1.
- Jellinek, A.M., Manga, M., Saar, M.O., 2004. Did melting glaciers cause volcanic eruptions in eastern California? Probing the mechanics of dike formation. J. Geophys. Res. 109, B09206. https://doi.org/10.1029/2004/B002978.
- Jiang, H., Lee, C.-T.A., Morgan, J.K., Ross, C.H., 2015. Geochemistry and thermodynamics of an earthquake: a case study of pseudotachylites within mylonitic granitoid. Earth Planet. Sci. Lett. 430, 235–248. https://doi.org/10.1016/j.epsl. 2015.08.027
- Keller, C.B., Schoene, B., Barboni, M., Samperton, K.M., Husson, J.M., 2015. Volcanic-plutonic parity and the differentiation of the continental crust. Nature 523, 301–307. https://doi.org/10.1038/nature14584.
- Kennett, J.P., McBirney, A.R., Thunell, R.C., 1977. Episodes of Cenozoic volcanism in the circum-pacific region. J. Volcanol. Geotherm. Res. 2, 145–163. https://doi. org/10.1016/0377-0273(77)90007-5.
- Kiipli, T., Hints, R., Kallaste, T., Verš, E., Voolma, M., 2017. Immobile and mobile elements during the transition of volcanic ash to bentonite an example from the early Palaeozoic sedimentary section of the Baltic Basin. Sediment. Geol. 347, 148–159. https://doi.org/10.1016/j.sedgeo.2016.11.009.
- Kirsch, M., Paterson, S.R., Wobbe, F., Ardila, A.M.M., Clausen, B.L., Alasino, P.H., 2016. Temporal histories of Cordilleran continental arcs: testing models for magmatic episodicity. Am. Mineral. 101, 2133–2154. https://doi.org/10.2138/am-2016-5718.
- Kistler, R.W., Wooden, J.L., Morton, D.M., 2003. Isotopes and ages in the northern Peninsular Ranges batholith, southern California (USGS Numbered Series No. 2003–489). Open-File Report. U.S. Geological Survey, Reston, VA.
- Lackey, J.S., Valley, J.W., Chen, J.H., Stockli, D.F., 2008. Dynamic magma systems, crustal recycling, and alteration in the central Sierra Nevada batholith: the oxygen isotope record. J. Petrol. 49, 1397–1426. https://doi.org/10.1093/petrology/egn030.
- Lee, C.-T.A., Morton, D.M., Kistler, R.W., Baird, A.K., 2007. Petrology and tectonics of Phanerozoic continent formation: From island arcs to accretion and continental arc magmatism. Earth Planet. Sci. Lett. 263 (3), 370–387. https://doi.org/10.1016/ j.epsl.2007.09.025.
- Lee, C.-T.A., Bachmann, O., 2014. How important is the role of crystal fractionation in making intermediate magmas? Insights from Zr and P systematics. Earth Planet. Sci. Lett. 393, 266–274. https://doi.org/10.1016/j.epsl.2014.02.044.
- Lee, C.-T.A., Jiang, H., Ronay, E., Minisini, D., Stiles, J., Neal, M., 2018. Volcanic ash as a driver of enhanced organic carbon burial in the Cretaceous. Sci. Rep. 8, 4197. https://doi.org/10.1038/s41598-018-22576-3.

- Liu, S., Nummedal, D., Liu, L., 2011. Migration of dynamic subsidence across the Late Cretaceous United States Western Interior Basin in response to Farallon plate subduction. Geology 39, 555–558. https://doi.org/10.1130/G31692.1.
- Lund, D.C., Asimow, P.D., 2011. Does sea level influence mid-ocean ridge magmatism on Milankovitch timescales? Geochem. Geophys. Geosyst. 12, Q12009. https:// doi.org/10.1029/2011GC003693.
- Martínez Ardila, A.M., Paterson, S.R., Memeti, V., Parada, M.A., Molina, P.G., 2018.
 Mantle driven Cretaceous flare-ups in Cordilleran arcs. Lithos 326–327, 19–27.
 https://doi.org/10.1016/i.lithos.2018.12.007.
- Miggins, D.P., Blome, C.D., Smith, D.V., 2004. Preliminary 40Ar/39Ar geochronology of igneous intrusions from Uvalde County, Texas: defining a more precise eruption history for the southern Balcones volcanic province (USGS Numbered Series No. 2004–1031). Open-File Report. U.S. Geological Survey, Reston, VA.
- Minisini, D., Eldrett, J., Bergman, S.C., Forkner, R., 2018. Chronostratigraphic framework and depositional environments in the organic-rich, mudstone-dominated Eagle Ford Group, Texas, USA. Sedimentology 65, 1520–1557. https://doi.org/10.1111/sed.12437.
- Namayandeh, A., Modabberi, S., López-Galindo, A., 2020. Trace and rare Earth element distribution and mobility during diagenetic alteration of volcanic ash to bentonite in eastern Iranian bentonite deposits. Clays Clay Miner. 68, 50–66. https://doi.org/10.1007/s42860-019-00054-9.
- Paterson, S.R., Ducea, M.N., 2015. Arc magmatic tempos: gathering the evidence. Elements 11, 91–98. https://doi.org/10.2113/gselements.11.2.91.
- Pearce, J.A., Norry, M.J., 1979. Petrogenetic implications of Ti, Zr, Y, and Nb variations in volcanic rocks. Contrib. Mineral. Petrol. 69, 33–47. https://doi.org/10.1007/BF00375192.
- Pearce, J.A., Harris, N.B.W., Tindle, A.G., 1984. Trace element discrimination diagrams for the tectonic interpretation of granitic rocks. J. Petrol. 25, 956–983. https:// doi.org/10.1093/petrology/25.4.956.
- Pierce, J.D., Ruppel, S.C., Rowe, H., Stockli, D.F., 2016. Zircon U-Pb Geochronology and Sources of Volcanic Ash Beds in the Upper Cretaceous Eagle Ford Shale, South Texas. Gulf Coast Assoc. Geol. Soc. J. 5, 253–274.
- Saleeby, J.B., Sams, D.B., Kistler, R.W., 1987. U/PB zircon, strontium, and oxygen isotopic and geochronological study of the southernmost Sierra Nevada Batholith, California. J. Geophys. Res. 92, 10443–10466. https://doi.org/10.1029/IB092iB10p10443.
- Scheidegger, K.F., Kulm, L.D., 1975. Late Cenozoic volcanism in the Aleutian Arc: information from ash layers in the northeastern Gulf of Alaska. Geol. Soc. Am. Bull. 86, 1407-1412.
- Scheidegger, K.F., Jezek, P.A., Ninkovich, D., 1978. Chemical and optical studies of glass shards in Pleistocene and Pliocene ash layers from DSDP Site 192, Northwest Pacific Ocean. J. Volcanol. Geotherm. Res. 4, 99–116. https://doi.org/10. 1016/0377-0273(78)90031-8.
- Sullivan, D.L., Brandon, A.D., Eldrett, J., Bergman, S.C., Wright, S., Minisini, D., 2020. High resolution osmium data record three distinct pulses of magmatic activity during cretaceous Oceanic Anoxic Event 2 (OAE-2). Geochim. Cosmochim. Acta 285, 257–273. https://doi.org/10.1016/j.gca.2020.04.002.
- Tang, M., Lee, C.-T.A., Chen, K., Erdman, M., Costin, G., Jiang, H., 2019. Nb/Ta systematics in arc magma differentiation and the role of arclogites in continent formation. Nat. Commun. 10, 235. https://doi.org/10.1038/s41467-018-08198-3.
- Winchester, J.A., Floyd, P.A., 1977. Geochemical discrimination of different magma series and their differentiation products using immobile elements. Chem. Geol. 20, 325–343. https://doi.org/10.1016/0009-2541(77)90057-2.
- Zartman, R.E., 1977. Geochronology of some alkalic rock provinces in eastern and central United States. Annu. Rev. Earth Planet. Sci. 5, 257–286. https://doi.org/10.1146/annurev.ea.05.050177.001353.